# NUMERICAL SOLUTION FOR GATE INDUCED VIBRATION DUE TO UNDER FLOW CAVITATION

*S. A. Sadrnezhad*

*Dept. of Civil Eng., K. N. Toosi University of Technology*
*Tehran, Iran, sadrnejad@hotmail.com*

**(Received: April 7, 1999 - Accepted in Final Form: April 5, 2001)**

**Abstract** Among the many forces to which hydraulic structures are exposed to, the forces induced by cavitation incident are of typical hydrodynamic unknown forces. The aim of this study is to define these forces as coupled fluid-structure interaction under two dynamic effects. The first dynamic effect which incorporates facilities for dealing with cavitation fluid is based on the appearance and bursting of vapor bubbles. The second hydrodynamic effect is dynamic excitation mechanism of the structure. In fluid-structure interaction, both the structure behavior and fluid are considered linear. Fluids can take some tension the extent of which depends on concentration and size of micro bubbles present; nevertheless, if the absolute pressure drops to a value close to the vapor pressure of the fluid, bubbles are formed and cavitation phenomena occurs. In this paper a fixed-wheel gate under the head pressure of a reservoir is considered to be affected by under flow cavitation. Normally, partially opened gates induce energy dissipation resulting in high turbulence, causing negative pressure and cavitation at the back and this excites the gate vibration. Moreover, there are several mechanisms which may cause heavy, self-excited vibration. According to the proposed method, a time function presenting the oscillation and pressure fluctuation in the vicinity of gate lip is estimated. This estimation is based on the parameters obtained from a two dimensional solution of flow under the gate lip. Accordingly, periodic time variable nodal forces are calculated and applied to gate lip element nodes. A transient dynamic solution of the gate, while its lip is sustaining nodal forces is estimated as time function. The results for the most sever modal deformation of the structure time history of some critical elements and variation of equivalent force versus time are presented.

**Key Words** Cavitation, Induced Vibration, Finite Element, Equivalent Nodal Forces

ð¼«B®½j°nk¼µ º°o½¯ ð½ ¬±¼wBT½°BŸ o¼A pA »{B¯ º°o½¯ ,Bµ²pBw o¼ jn¼° »ñ½§°nk¼µ ºBµ°o½¯ -¼¼ nj **²k¼ña** -½§°A :Sw¼A o¼A °j K½B› nj¤B¼w ° ²pBw y ®Ÿnk¯¼A o¼A Rn±~¼°o½¯ -½A • ½oíU ™¼šdU -½A " kµ/j±{»« J±vd« -½«°j /j±{»« ¥æBe¬±¼wBT½°BŸ y ½k¼Q S¦î ³¼ o¼A -½A /Sw¼A nBh¼°B´¼BLe ¬k¼ŸoU pA »{B¯ »ñ½«B®½j o¼FU o¼A nBT-n,¤B¼w ° ²pBw y ®Ÿnk¯¼A»wno¼ nj/k½C»« j±]±¼²pBwnj ³¦æBe SŸoe ° ²pBw»ñ½«B®½j ð½odU pA »{B¯ o¼A ° B´¼BLe qŸo²U ³¼³TV¼° »z®Ÿ½° y zŸ o¼o¼ nj ¤B¼w ³a o£A /Sw¼A ²k{ ³T-o£ oŠ¯ nj »† i °j oµ ¤B¼w ° ²pBw B´¼BLÇe ,j±ç{ oT²aŸ Sw¼A nBh¼nBz- ³¼ ð½jq¯ ³Ÿ »®¼í« ke pA ...½d« nj ™¦†« nBz- o£A B«A ,jn¼j no› B´¯Ç¶p¼k¯A foa³`½nj ð½ nm£o½p¬B½o] KLw ³¼ ~±-nB®Ç³§BŠ« -½A nj/jo½m0»« Rn±æ¬±¼wBT½°BŸ ²k½k0° ²k½j o£ ¥¼ñzU S§Be nj³`½nj»í¼L‡ n±†¼/Sw¼A ³T-o£ no› ¥¼¦dU jn±«,Sw¼A kw¬qh« pA »{B¯ nBz- ¤B²aîA SdU³Ÿ ¤±v®Ÿ¦ ³Ÿ³`½nj Sz0 nj »íƒ±« ° »¯Ç »–®« ºBµnBz-° ³T{Aj no› ³T–{Ç ¬B½o] pA »{B¯ y ½Bwo- ç oí« nj pB¼³2a¼¯ x BíUn¼° ºk] ð½odU WîB¼nB®Ç -½A »µB£/Sw¼A ²k{ ¥æBe³\¼T¯ nj,j±{»« ³`½nj»{BíUn¼A ð½odU³¼o\®« ³`½nj-½o½p³L§ »ñ½jq¯ nj nBz-R½o¼'U o¢¯B¼³Ÿ »¯B«p é¼BU ð½²k{ ³¼n¼A x°n t Bwk¼/j±{»« ³`½nj-½¢Bw o¼° ²k{ ¨B\¯A³`½nj o½p nj¬B½o] ºkí¼ °j ¥¼¦dU ºB®L« o¼ RBLwBd« -½A /Sw¼A ³T-o£ no› ³LwBd« jn±« Sw¼A ¥¼¦dU ð½/k¯²k{ ³LwBd« ³`½nj -½o½p·L§ ¶k¤µj ¥¼ñzU ¾q]A o¼ jn¼° »µo£ ºBµ°o½¯ »¼°B®U R½o¼'U B®L« -½A -½o¼k¼k{ S½B´ nj° ³Tz£ ³¼n¼A³`½nj -½o½p·L§ o¼ ¬B½o] pA »{B¯ J°B{ ºBµnB¼¤B²aîA ...½o{ nj¼nm£»ñ½«B®½j /Sw¼A ²k½jo£ ³¼n¼A»¯B«p ³`h½nBU Rn±~¼¬Ç °q]A° x BíUn¼A¤Be nj²pBw ºj±« ¥ñ{ o¼'U

## INTRODUCTION

In the normal case, when the absolute pressure at any point in the space occupied by flow reaches the vapor pressure pertaining to the prevailing temperature, vapor bubbles develop and voids filled with the vapor are formed in the fluid. Bubbles formed on the back surfaces of the gate edges and adhering to them due to the high speed whirl, may eventually reach points of relatively very high pressure. This effect will cause an explosion-like collapse ensues exerting a violent impact upon the surface adjacent to

the void. Of course, with conditions impairing, i.e. with increasing gate lip angle from zero upward, the space occupied by bubbles extends to downstream of the gate. The low pressure inside the bubbles leads to evaporation and explosion of the bubbles. As a result of continued bubble explosions, shock waves are created and move everywhere around. Metal surfaces exposed to cavitation, first loose their shininess and later on have spongy appearance. In addition to these corrosive effects, there will be gate vibration as well.

The conditions upon which bubbles are created were investigated by Kennard [1] and Hammitt [2]. Some research projects have been conducted on the damage to the surface of the structures by cavitation by Driels [3]. Bleich and Sandler [4] concluded that the effect of cavitation is similar to the one dimensional wave movement. The effect of cavitation such as shock effects on solid surfaces was mathematically shown by Newton [5]. Jones [6] assumed that the movement of created waves depends on the capacity of absorbed energy. A better assumption about the mechanism of bubble creation was presented by Johnson & Daily [7]. The time distance between two bubble explosions was investigated by Knapp [8]. The hereafter discussion is based on the last two references.

## PARAMETERS CONTROLLING CAVITATION UNDER THE GATE LIP

While a gate is semi-closed, and particularly, if no proper aeration is employed, the under flow may be unstable and turbulent after passing the gate lip. Under these circumstances, some hydrodynamic forces at the back of the gate make the vibration of gate body. The parameter showing the reduction of pressure is known as A [1], and can be calculated as follows:

$$A=\frac{C_c Y\ h}{V^2/2g}=\frac{-\Delta P}{\rho V^2/2g} \qquad (1)$$

where

h = the gate downstream pressure equal to($C_c$y+P).

V = Velocity.

g = Gravity acceleration.

$C_c$ = Coefficient of depth stability.

y = Coordinate in vertical direction.

Increasing parameter (A), increases the probability of cavitation. Usually, a general parameter is also introduced as K, which can be obtained as:

$$K=\frac{P\ p_v}{V^2/2g}=\frac{\Delta P+P_{atm}-p_v}{\rho V^2/2g} \qquad (2)$$

Where

P = Absolute pressure downstream of gate.

$P_{atm}$ = Atmosphere pressure.

$P_v$ = Vapor pressure.

Accordingly, A and K depend on each other. Basically, whenever, K is less than a certain value named as $K_c$, cavitation occurs. $K_c$ depends on the minimum value of $C_h$ at the vicinity of the gate which is introduced as cavitation parameter. Meanwhile, the geometry of gate lip can severely control the distribution of $C_h$, so wherever the value of $C_h$ is negative, cavitation will take place. However, parameters A and K, can show cavitation occurrence for a certain gate lip geometry with aeration, as follows:

$$\frac{p_i}{\rho V^2/2g}=(C_h)_{min}=A=\frac{Y\ C_c Y}{V_2/2g} \qquad (3)$$

where,

$$C_h=\frac{h_i-h}{V_i^2/2}$$

$h_i$ and h are piezometric heads at points i and j, respectively. The variation of $C_h$ is shown in Figure 1-a. $(C_h)_{min}$ is obtained for 21 types of gate lip geometries by Naudaschar et. al [9]. Figure 1-b shows the geometrical specifications of 21 types of gate lips. Variation of $(C_h)_{min}$ with relative gate opening shown in Figure 2-a,b [10,11].

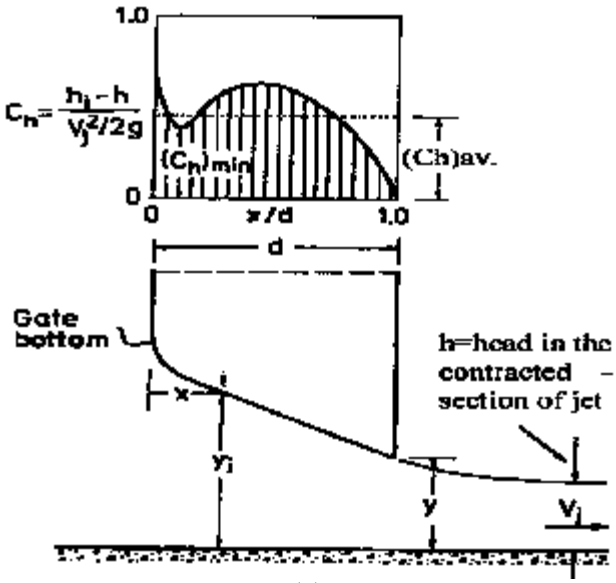


(a)

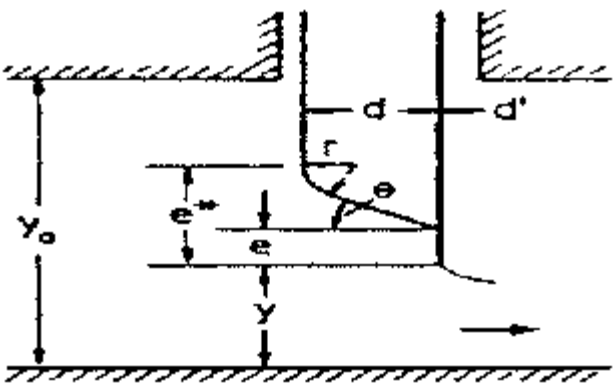


| Lip | θ (degrees) | r/d | e/d | e*/d | $y_o$/d |
|---|---|---|---|---|---|
| 1 | 45 | 0.4 | 0 | 1.07 | 5.0 |
| 2 | 30 | 0.4 | 0 | 0.81 | 5.0 |
| 3 | 20 | 0.4 | 0 | 0.64 | 5.0 |
| 4 | 0 | 0.4 | 0 | 0.40 | 5.0 |
| 5 | 0 | 0.4 | 0.15 | 0.55 | 5.0 |
| 6 | 0 | 0.4 | 0.20 | 0.70 | 6.0 |
| 7 | 0 | 0.4 | 0.45 | 0.85 | 6.0 |
| 8 | 0 | 0.4 | 0.60 | 1.0 | 6.0 |
| 9 | 0 | 0.2 | 0.15 | 0.35 | 6.0 |
| 10 | 0 | 0.2 | 0.30 | 0.50 | 6.0 |
| 11 | 0 | 0.2 | 0.45 | 0.65 | 6.0 |
| 12 | 0 | 0.6 | 0.30 | 0.90 | 6.0 |
| 13 | 0 | 0.6 | 0.45 | 1.05 | 6.0 |
| 14 | 20 | 0.4 | 0 | 0.81 | 4.0 |
| 15 | 0 | 0.4 | 0.45 | 0.85 | 4.0 |
| 16 | 0 | 0.2 | 0.15 | 0.35 | 4.0 |
| 17 | 30 | 0.4 | 0 | 0.81 | 8.0 |
| 18 | 0 | 0.4 | 0.45 | 0.85 | 8.0 |
| 19 | 0 | 0.2 | 0.15 | 0.35 | 8.0 |
| 20 | 30 | 0.4 | 0 | 0.81 | 12.0 |
| 21 | 30 | 0.4 | 0 | 0.81 | 20.0 |

(b)

**Figure 1**. (a) Variation of $C_h$ along gate thickness; (b) 21 types of gate lip geometries [8].

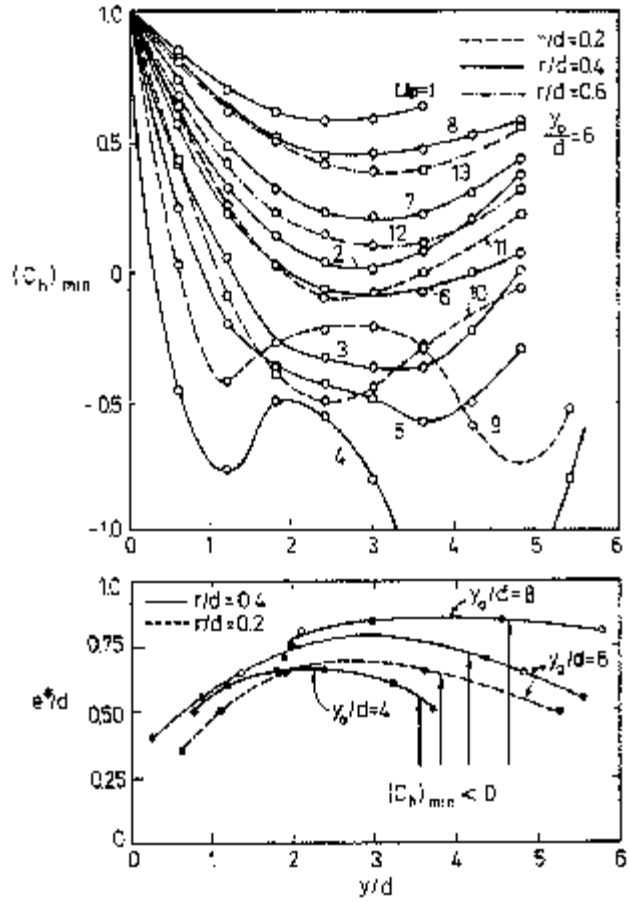


**Figure 2**. Variation of $(C_h)_{min}$.

## EQUILIBRIUMOF A SINGLE BUBBLE

Based on minimum energy level rule, the shape of a bubble must be sphere. This shape can guarantee the most stable condition of the bubble [2]. Therefore, the equilibrium of a half sphere bubble is sufficient to be considered. The following equation shows the equilibrium of tension forces at the cut edge of sphere and pressure forces inside the bubble.

$$\pi r^2 (p_{\cdot} + p_{\cdot}) = 2\pi r \varepsilon + \pi r^2 p_0 \tag{4}$$

or

$$p_{\cdot} \quad P_{\cdot} - \frac{2\varepsilon}{r} + P_0 \tag{5}$$

where

r = Sphere radius.

e stands for tension at the cut edge.

$P_0$ =External pressure.

$P_p + P_v$ = Pressure inside bubble.

Assuming that gas in the bubbles obeys the ideal gas law:

$$P_p = \frac{m R_g T_k}{\pi r^3} \quad (6)$$

$$P_i - P_v = \frac{A_g}{r^3} - \frac{2\varepsilon}{r} \quad (7)$$

where $$A_g = m R_g T_k / \pi \quad (8)$$

m = mass of gas.

$R_g$ = Universal gas constant.

$T_k$ = Absolute temperature.

The stability of the bubble can be investigated by solving the full differential equation [8] as follows:

$$\pi \left[ r \frac{d^2 r}{dt^2} + (3/2)\left(\frac{dr}{dt}\right)^2 \right] = (P_0 - P_v - \frac{A_g}{r^3} - \frac{2\varepsilon}{r}) \quad (9)$$

Positive values of the right hand side of Equation 9 shows that the diameter of bubble is increasing. Conversely, if this value is negative, it shows that the bubble is decreasing in diameter. However, the right hand side represents a force which can change the bubble size. The stable bubbles exist while the right hand side is zero. This case leads to the validity of the following equation:

$$P_d - P_0 - P_v = (4/3)\left(\frac{2\varepsilon}{r_c}\right) \quad (10)$$

where,

$r_c$ = The critical value of r upon which the right hand side of Equation 9 is zero.

This equation can lead to obtaining a critical radius for stable bubbles.

$$r_c = (3/2)\left(\frac{m R_g T_k}{\pi \varepsilon}\right) \quad (11)$$

Therefore, at the time of severe condition of cavitation under the gate lip, the size of all bubbles are the same and are defined by $r_c$.

## CAVITATION UNDER GATE LIP

Several transient conditions take place while a gate starts moving up or down to control the flow in conduit. However, each time a pressure distribution can be provided by solving Navier-Stokes equations in three dimensional condition. Theoretically, any pressure distribution obtained can be led to the distribution of coefficient of cavitation. This coefficient can simply present if and where, there may be local or even a large zone of cavitation taking place.

To simplify the problem, only stable flow conditions are considered here. Therefore, to have stable size of bubbles, the right hand side of equation 9 must be equal to zero. The following equation can be employed to calculate the radius of stable bubbles.

$$r^3(P_i - P_v) + 2r^2\varepsilon - A_g = 0 \quad (12)$$

Also, Equation 10, can give the value of $P_d$. The localization of cavitation throughout the flow, specially in the vicinity of the gate lip, is the most important data. Accordingly, the effect of cavitation hydrodynamic forces must be applied to structural elements in the vicinity of cavitation region. Consequently, the most sever case is when the width of cavitation zone is equal to but against the gate lip. However, this condition may be known as the upper bound case of cavitation effect on the gate lip. Furthermore, following the upper bound case, the rows of the same size bubbles (radius r) in the most condensed possible form may be supposed to explode against the gate lip edge. The possible organized form of bubble rows upon assuming simultaneous and uniform bubbling is shown in Figure 3.

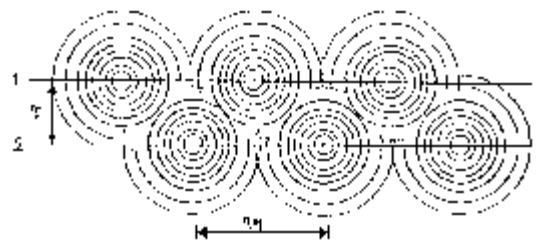

**Figure 3**. Proposed periodic made bubbles with rows in the most condensed form.

Normally, fluids can not sustain a shear wave. However, longitudinal waves in a liquid propagate at the speed of sound. The velocity of sound in an elastic fluid is directly proportional to the square root of the ratio of bulk modulus to the density of fluid. This velocity, Vs, is calculated as follows [7].

$$V_s = \left(\frac{B_m}{\rho_m}\right)^{1/2} \quad (13)$$

where,

$B_m$ = Bulk modulus of water containing some air.

$r_m$ = Density of water containing some air.

The above mentioned two parameters are calculated according to the equation presented in reference [7]. According to reference [7], the effects of shock wave decreases with the distance from bubble center. The shock wave velocity is equal to the speed of sound in water. Based on experiments [7], the pressure intensity at a distance, two times the initial bubble radius from the collapse center is about 200 times the ambient pressure at the collapse site. In the stated case the bubble diameter was 0.1 mm. and the mean bubble pressure reported to be equal 120.9 KPa [8].

Experimentally, it has been proven that the cavitation damages due to explosion shocks are much more than spherical preparing shocks. Furthermore, the intensity of pressure due to symmetric shocks is much more than non-symmetric ones. According to experiments, the wave velocity of non-symmetric producer is half the sound velocity in water. As a result, following the most sever case, it may be supposed that rows of the same size bubbles explode simultaneously and regularly. Certainly, this case can create more sever condition than irregularity of bubbles. These assumptions lead to the condition of bubbles explosions to the variation of pressure due to the large number of vortices made by each bubble explosion. The time distance between two consequent rows in the most sever cavitation is equal to the time which must be spent for replacing the next row of explosion. The length of this distance may be assumed as the minimum distance between two consequent rows whose periods are 90° away from each other. Two consequent such rows are shown in Figure 3.

## HARMONICEQUIVALENTNODAL FORCES OF CAVITATION

The distribution of periodic variation of pressure obtained by bubble explosions is assumed to be a function of location and time. Adopting that the most cavitation effects are applied to the gate-lip edge elements, the variation of obtained pressure must be changed into equivalent nodal forces. However, a better assumption is that pressure effects are applied along the lower edges of the nearest row of the element adjacent to the starting points of cavitation. In a three dimensional case, the components of equivalent nodal forces representing pressure variation are the function of time. Among those components the one perpendicular to gate leaf is the most effective one to make the gate vibrate. Of course, one or two or even all three components can be considered to compute the gate vibration. The created periodic distributed pressure along the gate-lip edge perpendicular to the gate leaf in the first mode may be written as follows:

$$P_y = \left(\frac{P_{max} - P_{min}}{Vt/R}\right) \sin\left(\frac{\pi x}{4r}\right) \quad (14)$$

where,

V = The velocity of flow under the gate lip.

t = Time.

x = Horizontal distance along the gate lip.

R = The distance axis to axis of two adjacent rows of exploding bubbles.

The equivalent nodal forces for the first and second modes are calculated as follows:

$$f_y = \int_{L_e} N^T \left(\frac{P_{max} - P_{min}}{\pi Vt/R}\right) \sin\left(\frac{\pi x}{4r}\right) dx \quad (15)$$

$$f_e = \int_{l_e} N^T \left(\frac{P_{max} - P_{min}}{\pi V t / R}\right) \cos\left(\frac{\pi 4}{4r}\right) \quad (16)$$

Employing rectangular isoparametric elements and linear shape functions, leads to the equivalent nodal forces for two modal forces as follows:

$$f_y = \begin{Bmatrix} f_{y_1} \\ f_{y_2} \end{Bmatrix} = \left[ \int_0 N^T \alpha \{ \sin\beta \sin\gamma \cos\beta (\cos\gamma - (1/\gamma)\sin\lambda) dx - \cos\beta (\cos\gamma - (1/\gamma)\sin\lambda) dx \right.$$

$$f_e = \begin{Bmatrix} f_{y_1} \\ f_{y_2} \end{Bmatrix} = \left[ 2 \int_{l_1} N^T \alpha \{ \cos\beta \sin\gamma \sin\beta (\cos\gamma + (1/\gamma)\sin\lambda) dx - \sin\beta (\cos\gamma + (1/\gamma)\sin\lambda) dx \right.$$

where,

$$\alpha = 8r\left(\frac{P_{max} - P_{min}}{\pi V t / R}\right)$$

$$\beta = \frac{\pi(y_1 + y_2)}{8r} \quad , \quad \gamma = \frac{\pi l_e}{8r}$$

$y_1$ and $y_2$ = Coordinate of the first and last nodes on the elements edge.

$l_e$ = The length of element edge receiving cavitation effects.

The calculated equivalent nodes forces are applied to the nodes on the gate-lip edge where cavitation takes place.These nodal forces also change with respect to time. Assuming a regular and simultaneous bubble explosions along each row against the whole gate-lip edge, the following equation presents the variation of each nodal force versus time.

$$f_t = (f_{ymax} - f_{ymin}) \sin\left(\frac{2\pi t}{\tau}\right) \quad (19)$$

where,

$f_t$ = Equivalent nodal force as a function of time.

t = The time between two consequent row explosions.

$f_{min}$ , $f_{max}$ = Minimum and maximum values of $f_y$.

To apply this nodal force to the gate lip edge, it can be divided into a constant amplitude and a time function factor.

## DYNAMICRESPONSE OF PLATES SUBMERGED IN WATER

While a flat shape structure is to vibrate and submerged fully in water or even only one side of it is in contact in water, fluid-structure interaction is known to affect as a damper, though, the natural frequency is less than the free vibration in air. An alternative approach is to evaluate the added mass term instead of considering damping effects through fluid-structure interaction. Many authors recommended different added mass factors to adjust the vibration of a flat structure in water [10], [11], [12], and [13].

In this study, to obtain a proper added mass for the plates submerged in water, a Lagrangian finite element solution is employed to solve the effect of fluid-structure interaction in vibration of a single plate [14]. To provide a numerical model of a single plate and surrounding water, the behavior of both plate and water is assumed as linear elastic with corresponding K'(bulk modulus) and G(shear modulus). These parameter values for water need some investigation, although, G is not to be taken as zero and v (Poisson ratio) not to be greater than or equal to 0.5. Furthermore, natural frequencies obtained through different G values are severely different!

Two types of the composition of elements including steel shells in solid waters (type 1), and steel solid waters (type 2) were investigated [14]. For a plate vibration submerged in water, the general dynamic equation is as follows:

$$(M + A')\ddot{\delta}_i + (C - B')\dot{\delta}_i + (K + C')\delta_i = F_i(t) \quad (20)$$

where,

M, C, and K are mass, damping, and stiffness matrices respectively.

A', B', and C' are similar to M, C, and K, respectively, but as the effects of submerging

the system in water. $\ddot{d}_i$ , $\dot{d}_i$ and $d_i$ are acceleration, velocity and displacement respectively. $F_i(t)$ stands for hydrodynamics force applied to node i which is naturally a function of t (time).

Accordingly, the natural frequency of a plate in the case of submerging in the water ($f_{nw}$) is calculated as follows:

$$f_{nw} = \frac{1}{2\pi}\sqrt{\frac{K+C'}{M+A'}} \qquad (21)$$

Therefore, assuming $f_n$ as the natural frequency of plate in air, the ratio of the two frequencies is calculated as follows:

$$\frac{f_{nw}}{f_n} = \sqrt{\frac{1}{1+(A_x/m_x)}} \qquad (22)$$

where, $A'_x$ and $m_x$ are added mass because of submerging and mass itself for unit length of plate at nth mode, respectively.

The Struhal hydrodynamic force affecting a flat body while water is passing by it, is calculated as follows:

$$f_f = \frac{SV_0}{d} \qquad (23)$$

where,
$f_f$ = Struhal hydrodynamic force.
S = Strouhal number.
$V_0$ = Approach velocity in flow path.
d = Thickness of body perpendicular to flow.
Strouhal number depends on section geometry of plate.

$F_i(t)$ in the right hand side of Equation 20 comprises a vertex shedding-induced hydrodynamics force and a variable Struhal force of which the frequency stated in Equation 23. The drag force can be calculated as follows:

$$F_{d,s} = C_{d,s} lD \left\{\frac{\sin\alpha}{\sin\beta}\right\}^{1/2} \rho \frac{V^2}{2g} \qquad (24)$$

where,
$C_{d,s}$ depends on the geometry of plate.
a and b = Flow angle and plate angle respectively.
r and n stand for density and flow velocity.
D= Thickness of body perpendicular to flow.
l = The length of body in the flow.

In this study it has been assumed that all plates (skin plate, stiffeners, and flanges) participating in gate structure are fully submerged in water. Certainly, while the gate body is partly submerged in water, the investigated added mass must be considered only for submerged elements. In the case of some plates to be one sided submerged in water, new investigation must be carried out to obtain rationalized added mass.

## NUMERICALRESULTS

To show the applicability of the proposed method, one segment of a bulkhead gate composed of four segments, is chosen. This segment is 5.8m. wide, 2.70m. high and 0.60m. thick. The maximum head for this upstream sealed gate is 45m. of water. The material used in manufacturing the gate was ST-44-2, and the skin plate 30mm thick. According to the general observations conformed with the equation given for rc, the average diameter of bubbles created by cavitation is assumed to be 0.2mm. The maximum pressure along each bubble row in exploding condition is considered as 200 times of minimum pressure on the same row.

These assumptions will lead to a pressure variation along the gate-lip edge as follows:

$$P = 199 \times 120.9 \sin\left(\frac{\pi x}{0.0002}\right) \qquad (25)$$

Results of solving Navier-Stokes equation upon two dimensional condition to find an average pressure and velocity under gate lip elements is shown in Figure 4-a. In this Figure the finite element mesh, suction and probable cavitation zone are shown. Figure 4-b and 4-c show the variation of time function f(t) which are two simulated sinusoidal and cosine based change of pressure fluctuation under the gate lip. The flow lines are shown in Figure 4-b.

Figure 5-a shows the maximum deformed

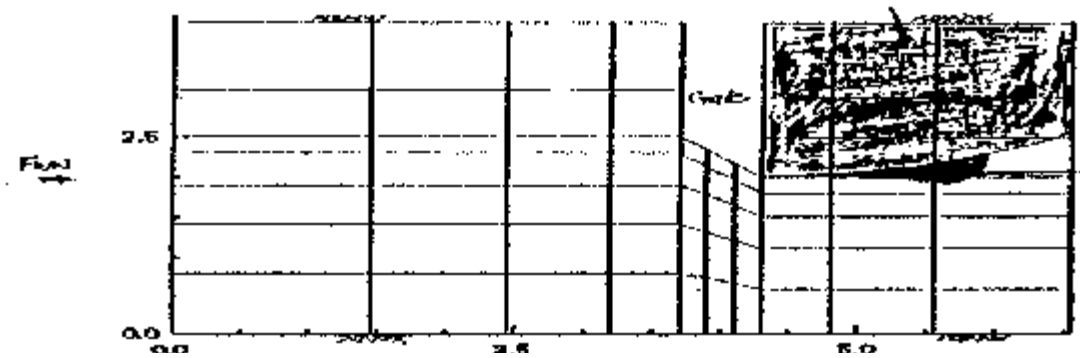


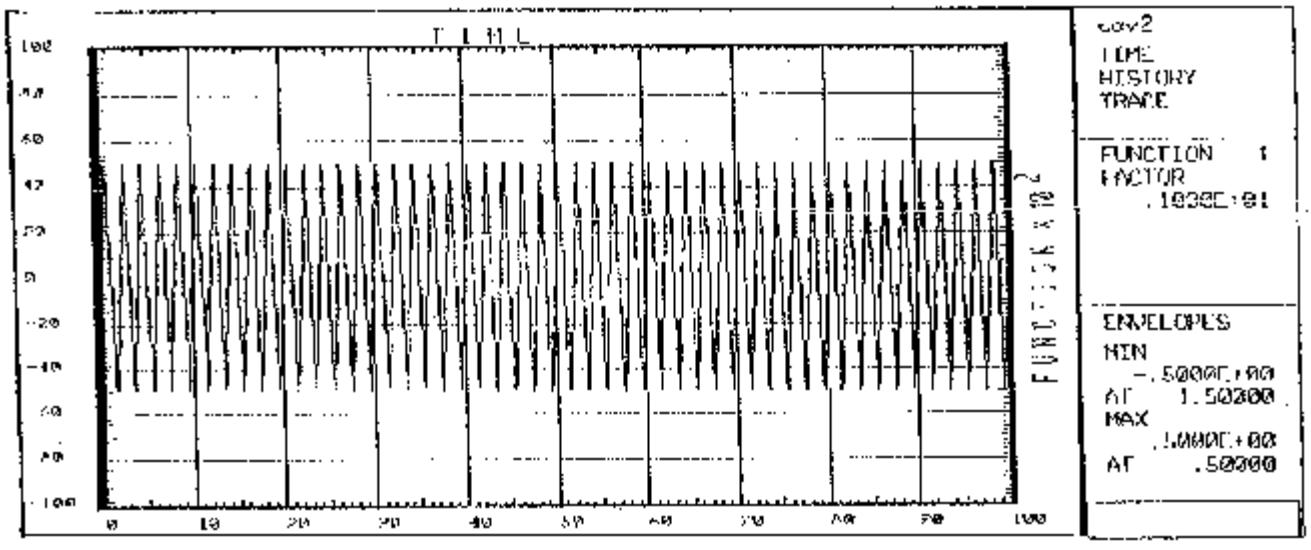


**Figure 4-b**. Sinusoidal Time function f(t) pressure fluctuation under the gate lip.

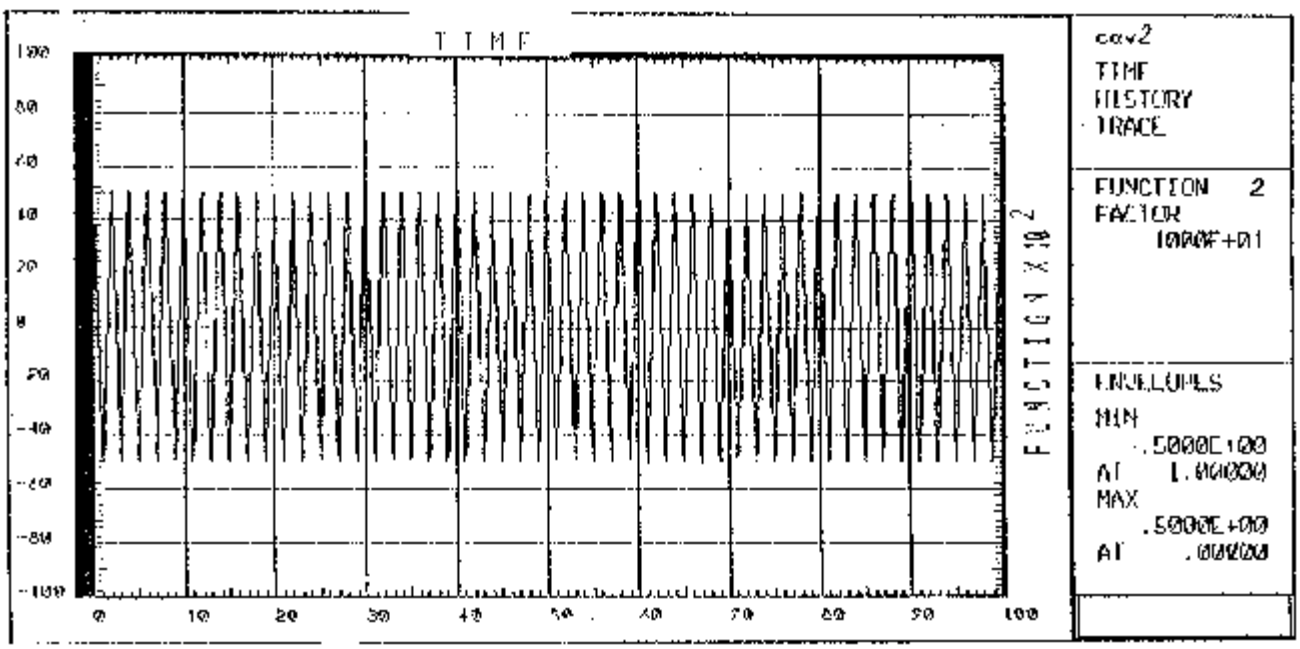


**Figure 4-c**. Cosine base Time function f(t) pressure fluctuation under the gate lip.

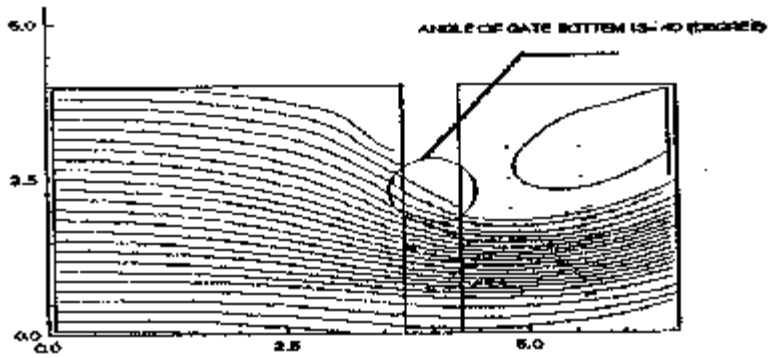


**Figure 4-d**. Stream lines.

mesh, the stress contours of cavitation effects during the gate vibration. svm (combined stress) during the vibration of gate under on the gate due to two time functions are shown in Figures 5-b and 5-c. The maximum stresses are 3990 and 3490 N/mm$^2$ respectively. These stresses are obviously, more than the allowable stress which according to DIN 19704 [12] is 1730 N/mm$^2$.

However, despite omitting the normal pressure on the gate, the existing stress is nearly twice as the allowable stress.

Deformed shapes of the gate under the two employed time functions are shown in Figure 5-d and 5-e respectively.

Figure 6-a, b, and c present time histories of deformation, velocity and acceleration for the most sever node (node No.11).

## CONCLUSIONS

As a numerical solution, the presented method can be employed to carry out the intensity of vibration of gate due to cavitation from the lowest value extending up to the most sever one.

The proposed method is also an extension of the simple, approximate, traditional added-mass solution for which any general-purpose structural analysis can be utilized. This method was employed to determine the dynamic behavior of gate including fully and partly submerged plates upon cavitation effects.

It is shown numerically, that under the most sever condition of cavitation, additional stresses up to twice the maximum existing stress may be created in the structure of the gate. Furthermore, time histories for deformation, velocity and acceleration of any critical zone may be obtained to control fatigue effects and probability of cracking.

According to the procedures represented by this method, one can also, predict the effect of any local, non-symmetric, or even close/far zone of cavitation to the gate body.

To clarify the reliability of the method further, the results must be compared with some hydraulic model tests.

## REFERENCES

1. Kennard, E. H., "Cavitation in an Elastic Liquid", ***The Physical Review***, Vol. 65, Nos. 5 and 6, (1943), 172-181.
2. Hammitt, F. G., "Cavitation and Multi Phase Flow Phenomena", McGraw Hill, 1980.
3. Driels, M. R., "The Effect of a Nonzero Cavitation Tension on the Damage Sustained by a Target Plate Subjected to an Underwater Explosion", ***J. Sound and Vibration***, Vol. 73, No. 4, (1980), 533-545.
4. Bleich, H. H. and Sandler, I. S., "Interaction Between Structures and Bilinear Fluids", ***Int. J. of Solid and Str.***, Vol. 6, (1970), 617-639.
5. Newton, R. E., "Finite Element Study of Shock Induced Cavitation", ***ASCE, Spring Convention, Portland Oregon***, (April 1980), 1-34.
6. Jones, A. V., "Coolant Cavitation in Dynamic Containment Loading", ***Nuclear Engineering and Design***, Vol. 55, (1979), 197-206.
7. Daily, J. W. and Johnson, V. E., "Jr. Turbulence and Boundary Layer Effects on Cavitation Inception from

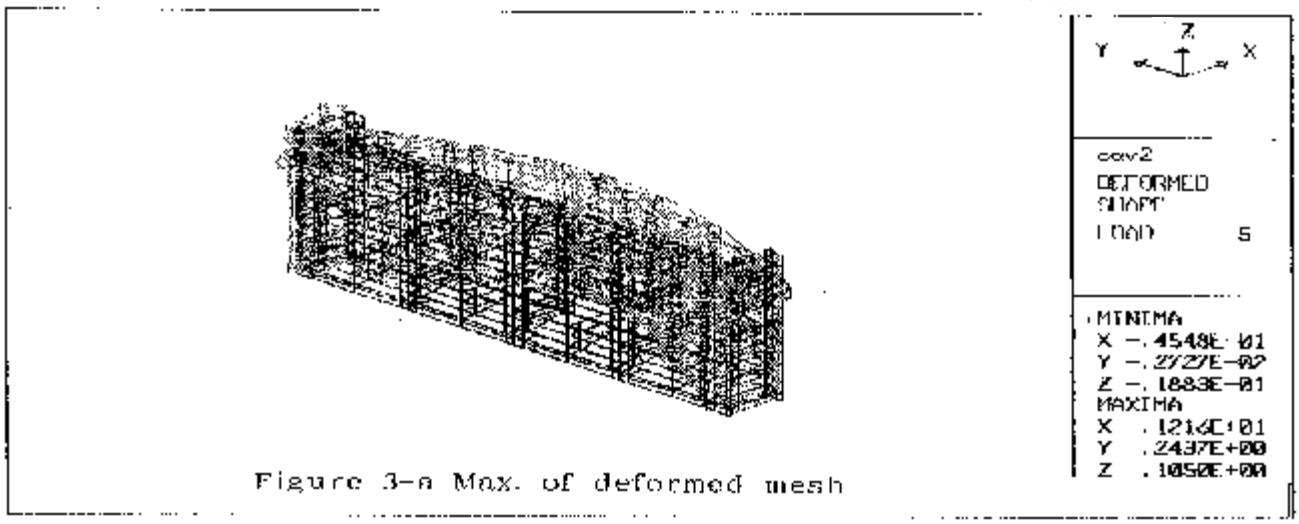


Figure 3-a Max. of deformed mesh

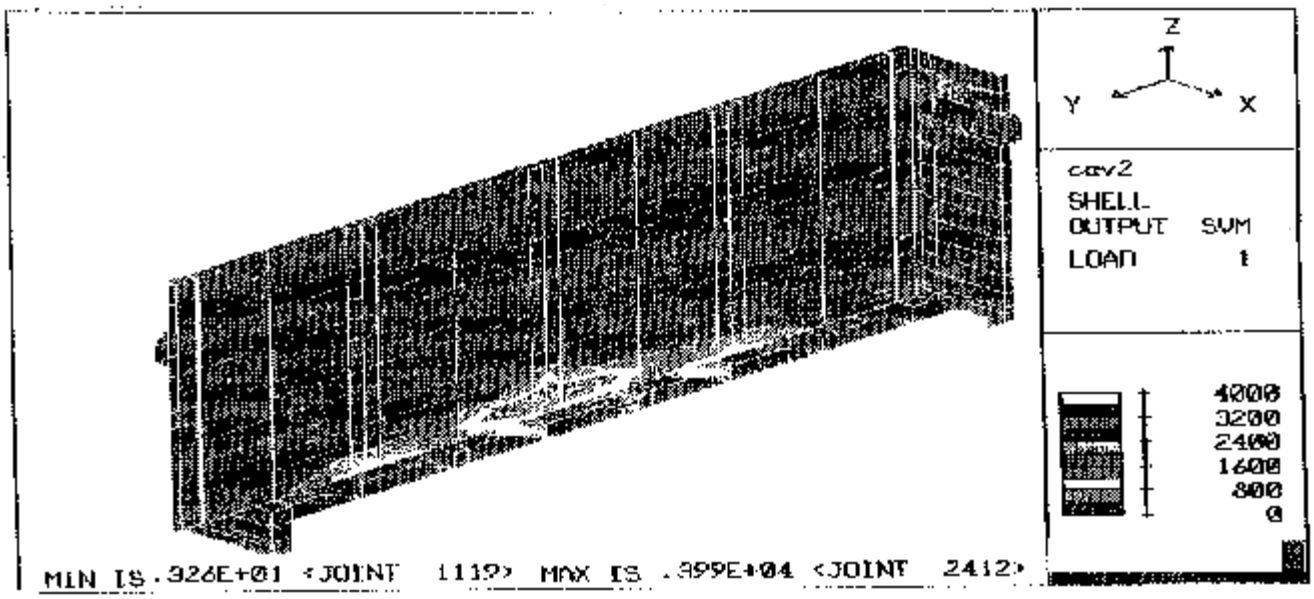


**Figure 5-b**. $S_{vm}$ stress contours due to Sine time function.

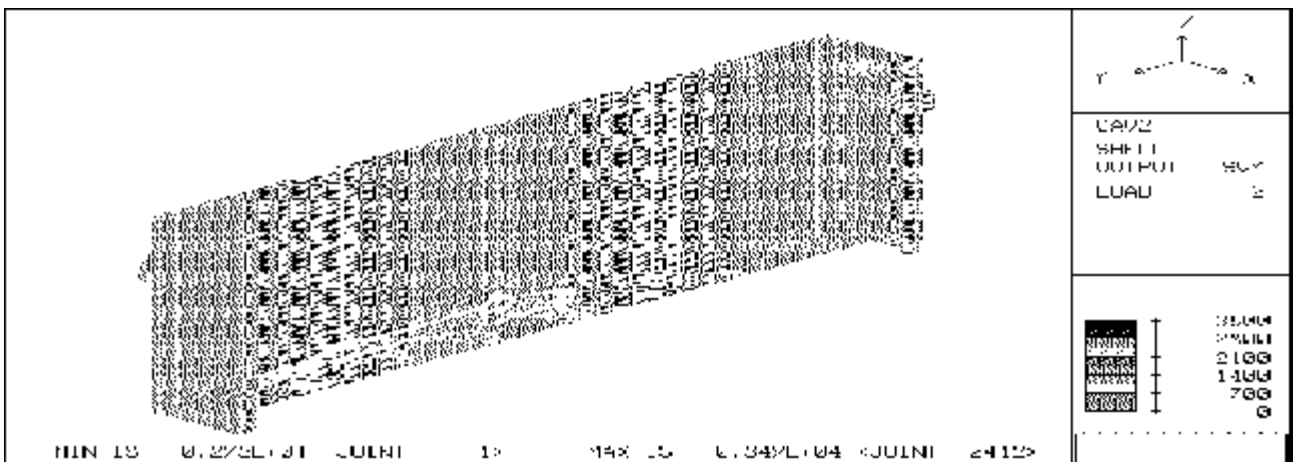


**Figure 5-c**. $S_{vm}$ stress contours due to Cosine time function.

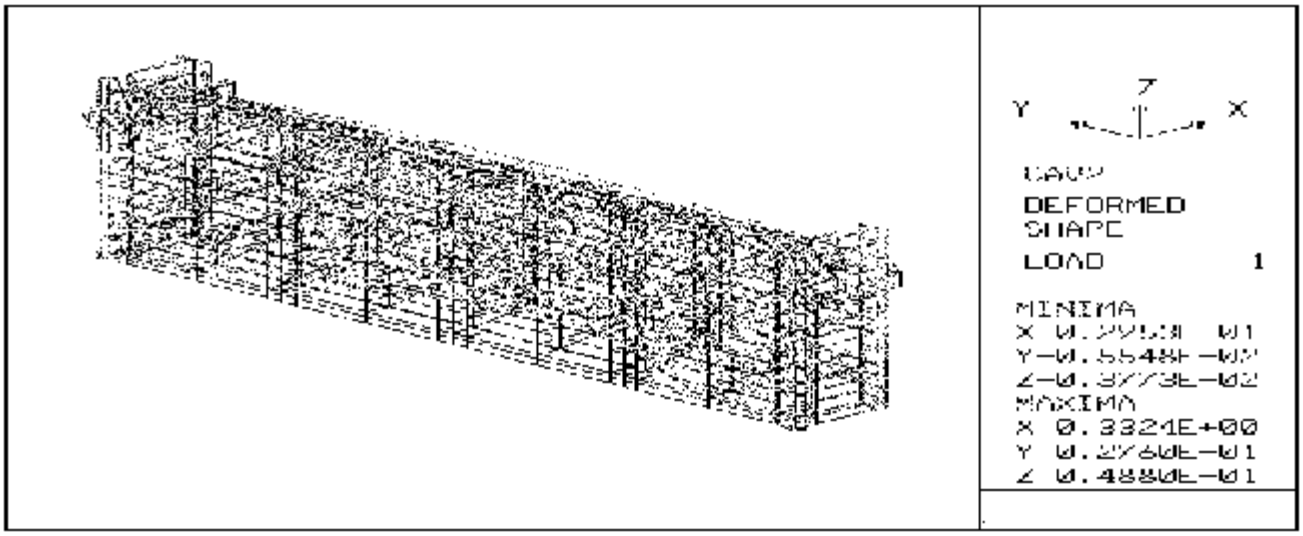


**Figure 5-d**. Deformed mesh due to Sine time function.

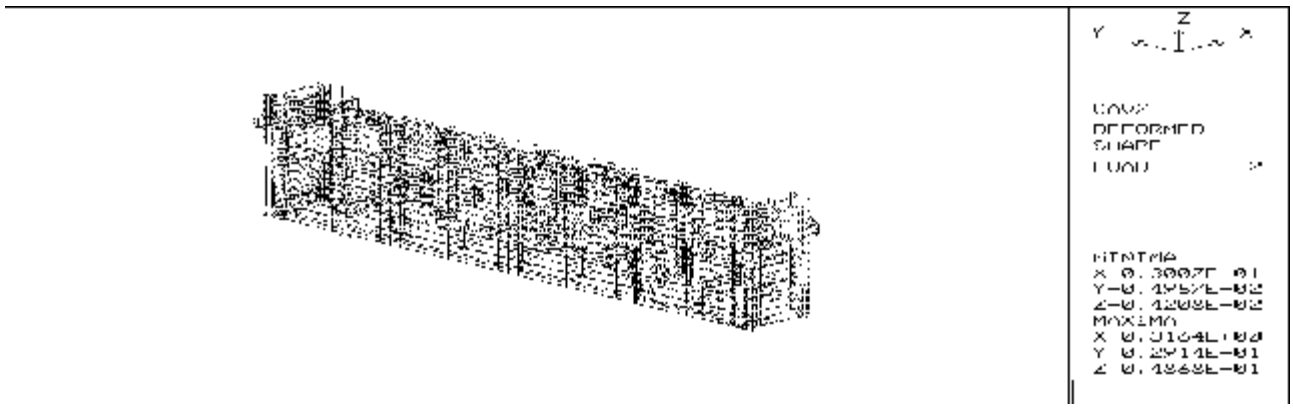


**Figure 5-e**. Deformed mesh due to Cosine time function.

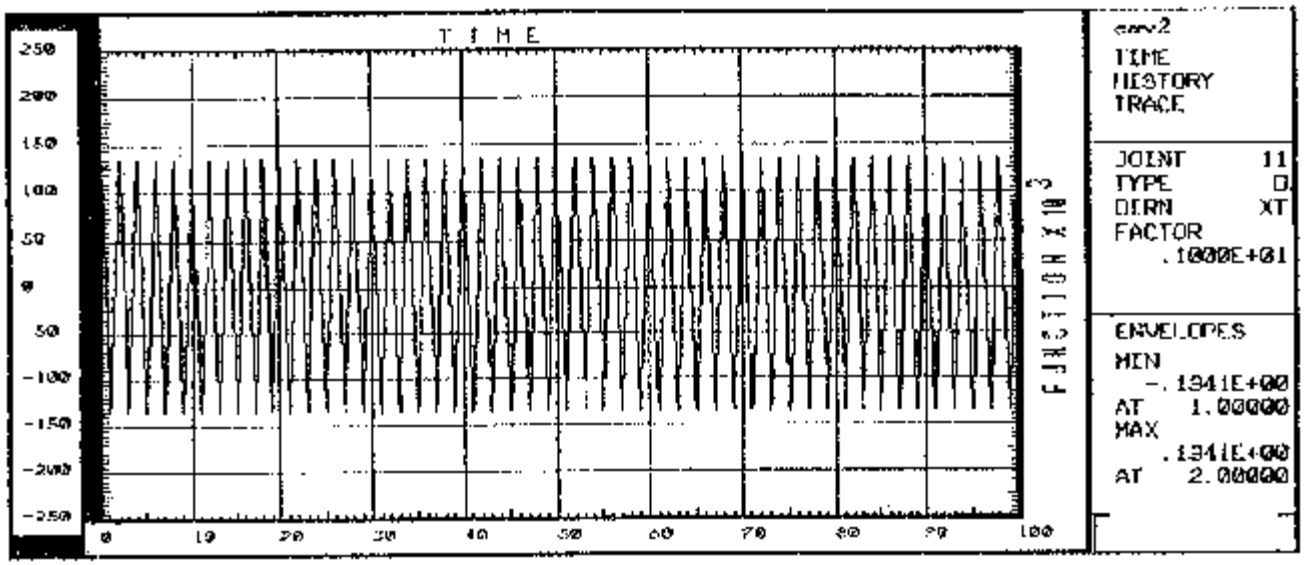


**Figure 6-a**. Deformation Time history of Node 11.

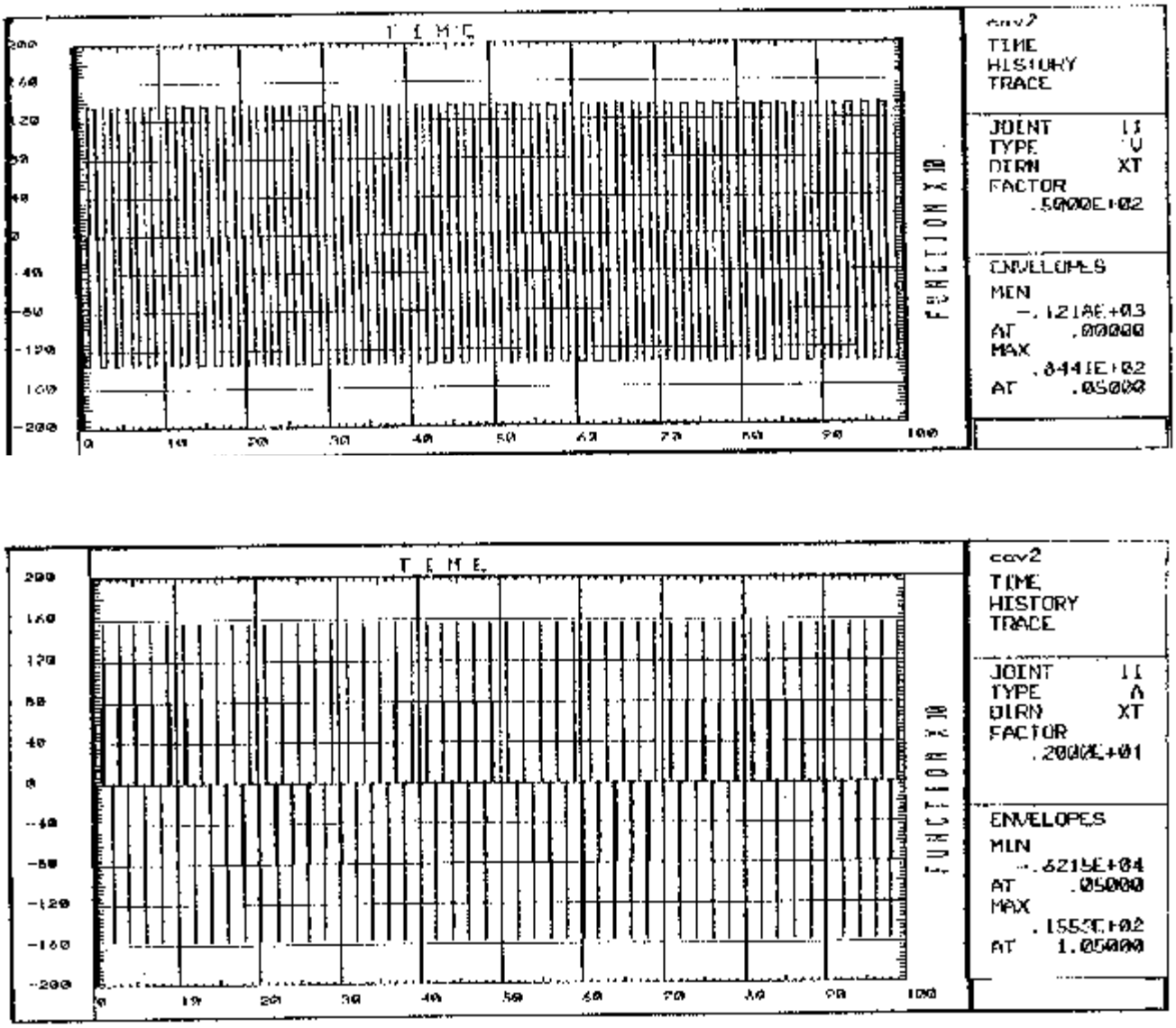


**Figure 6-c**. Acceleration Time history of Node 11.


Gas Nuclei", ***Transactions of the American Society of Mechanical Engineering*** Vol. 78, (1956), 1695-1706.

8. Knapp, R. T., Daily, J. W. and Hammitt, F. G., "Cavitation", McGraw Hill Inc., New York, NY, (1970).
9. DIN 19704, "Hydraulic Steel Structures, Criteria for Design and Calculation", Table 3, P. 11, (1972).
10. Westergaard, H. W., "Water Pressures on Dams During Earthquakes", ***Transactions ASCE***, Paper No. 1835, (1933).
11. Maheri, M. R. and Severn, R. T., "Impulsive Hydrodynamics Pressures in Ground-Based Cylindrical Structures", ***Journal of Fluids and Structures***, Vol. 3, (1989), 5-55-577.
12. Maheri, M. R. and Severn, R. T., "Experimental Added-Mass in Modal Vibration of Cylindrical Structures", ***Journal of EngineeringStructures***, Vol. 14, No.3, (1992), 163-175.
13. Nguyen, T. D., "Added Mass Behavior and its Characteristics at Sluice Gates", ***Proceeding of the BHRA International Conference on Flow-Induced Vibrations***, Reading, U.K., (Sep. 1982), 84-93.
14. Rasoolan, I., "Numerical Investigation of Trashrack Vibration Against Hydrodynamics Effects", MSc Theses, K. N. Toosi University of Technology, Tehran, Iran, (1998).